Westinghouse Non-Proprietary Class 3

WCAP-16158-NP
Revision 0

August 2008

Technical Basis for Repair Options for Reactor Vessel Head Penetration Nozzles and Attachment Welds: Beaver Valley Unit 2

WCAP-16158-NP
Revision 0

Technical Basis for Repair Options for Reactor Vessel Head Penetration Nozzles and Attachment Welds: Beaver Valley Unit 2

A. Udyawar

K. R. Hsu
S. Jirawongkraisorn
C. Y. Yang

August 2008

Verifier: C. K. Ng*
Piping Analysis and Fracture Mechanics

Approved: S. A. Swamy*
Manager, Piping Analysis and Fracture Mechanics

*Electronically approved records are authenticated in the Electronic Document Management System.

Westinghouse Electric Company LLC
P.O. Box 355
Pittsburgh, PA 15230-0355

TABLE OF CONTENTS

LIST OF TABLES

LIST OF FIGURES

1 INTRODUCTION

Leakage has been reported from the reactor vessel closure head penetration nozzles in a number of plants. This has led to requests for inspection of these regions. Inspections of the leaking penetrations indicate the presence of axial cracks that extend above and below the head penetration attachment welds. The cause of these axially oriented cracks has been determined to result from primary water stress corrosion cracking (PWSCC) that are driven by both steady state operating and residual stress. [

]^{a,c,e}

As a part of the inspection and repair efforts associated with the head penetration inspection program for Beaver Valley Unit 2, engineering evaluations were performed to support the repair efforts. The purpose of this report is to provide the technical basis for the use of the embedded flaw repair method if indications or flaws are found in a head penetration nozzle and attachment weld during the Beaver Valley Unit 2 vessel head inspections. [

]^{a,c,e} The methodology used is based on extensive analytical work completed to-date for the Westinghouse Owners Group (WOG), and a large collection of test data obtained under the sponsorship of Westinghouse, Babcock & Wilcox (B&W) and Combustion Engineering Owners groups (CEOG), as well as the Electric Power Research Institute (EPRI).

[

]^{a,c,e} Engineering evaluations were performed to determine the maximum flaw sizes that would satisfy the requirements in Section XI of the ASME Code [1] and be suitable to support the weld repair process. The results presented in this report would enable the weld repair team to effectively determine the appropriate repair method.

Section XI repair rules allow the use of grinding to remove flaws, regardless of the edition of the Code. The only requirement is to ensure that the excavated region still meets the stress limits of the original construction code, which was Section III. Evaluations were performed to address the potential local structural discontinuities that would result from grinding operations performed to excavate flaws in the head penetration nozzles.

In this report, the technical basis to support the use of the embedded flaw repair method for a flawed Control Rod Drive Mechanism (CRDM) penetration is provided in Section 2. The technical basis that supports a similar application for a flawed head penetration attachment weld is provided in Section 3. The results of the evaluation to provide a basis for grinding operations to excavate flaws are discussed in Section 4.

Note that there are several locations in this report where proprietary information has been identified and bracketed. For each of the bracketed locations, the reason for the proprietary classification is given, using a standardized system. The proprietary brackets are labeled with three different letters to provide this information and the explanation for each letter is given below:

a. The information reveals the distinguishing aspects of a process or component, structure, tool, method, etc., and the prevention of its use by Westinghouse's competitors, without license from Westinghouse, gives Westinghouse a competitive economic advantage.

c. The information, if used by a competitor, would reduce the competitor's expenditure of resources or improve the competitor's advantage in the design, manufacture, shipment, installation, assurance of quality, or licensing of a similar product.

e. The information reveals aspects of past, present, or future Westinghouse or customer funded development plans and programs of potential commercial value to Westinghouse.

2 TECHNICAL BASIS FOR APPLICATION OF EMBEDDED FLAW REPAIR TECHNIQUE TO CRDM PENETRATION NOZZLES

This section provides a discussion on the technical basis for the use of embedded flaw repair method for a flawed head penetration nozzle. [

]^{a,c,e} Flaw evaluations for postulating planar flaws with various flaw sizes in the head penetration nozzles were performed. [

]^{a,c,e}

2.1 Acceptance Criteria

The evaluation procedures and acceptance criteria for indications in austenitic piping are contained in paragraph IWB 3640 of ASME Section XI [1]. These criteria are directly taken from 2002 Addenda. [

a,c,e

The applicability of the [ ]^{a,c,e} used in Section XI was investigated based on a study of all the piping fracture experiments to date (about 3000) by the Working Group on Pipe Flaw Evaluation. It was determined that the [ ]^{a,c,e} become progressively more conservative as the pipe radius to thickness ratio gets smaller. Conversely, for pipes with thin walls, the [ ]^{a,c,e} can become non-conservative. Therefore, a limitation has been imposed by Appendix C of Section XI to limit its applicability to those pipes whose radius to thickness ratio is less than 15. Since the nozzle mean radius to thickness ratio for the CRDM penetration nozzles is about 2.7, the [ ]^{a,c,e} in Section XI is applicable to Beaver Valley Unit 2 CRDM penetration nozzles.

2.1.1 Acceptance Criteria for Axial Flaws

[

]^{a,c,e}

[

]a,c,e

This limit ensures that surface flaws would remain below the critical size [
]a,c,e

2.1.2 Acceptance Criteria for Circumferential Flaws

[

]a,c,e

[

]a,c,e

2.2 METHODOLOGY

The evaluation assumed that a flaw has been detected in a penetration nozzle and that the embedded flaw repair method is used to seal the flaw from further exposure to the primary water environment. The evaluation began with the determination of an allowable flaw size based on the acceptance criteria described in Section 2.1 for a flaw postulated in the penetration nozzle. [

]a,c,e The modified allowable flaw size was used to determine the maximum allowable flaw size that is acceptable using the embedded flaw repair method.

2.2.1 Geometry and Source of Data

There are many head penetration nozzles in the reactor vessel upper head. The outermost CRDM penetration nozzles (penetrations 58-65) were selected for analysis because [

]a,c,e A schematic of a closure head penetration nozzle for a typical Westinghouse design plant is shown in Figure 2-1. Table 4-1 shows the head penetration nozzle dimensions for Beaver Valley Unit 2. The distributions of residual, transient thermal, and pressure stresses in the vessel head penetration nozzle were obtained from detailed three-dimensional elastic-plastic finite element analysis [14]. The through-wall stress distributions from the finite element analysis were used to determine the maximum allowable flaw sizes and the fatigue crack growth for the CRDM penetration nozzles. [

]a,c,e The finite element model with the selected stress cuts is shown in Figure 2-2. A "stress cut" means an imaginary line or plane over which stress distribution is evaluated.

The regions of the head penetration that have the highest stresses are the ones closest to the attachment weld (Stress Cuts 1 and 2 in Figure 2-2). [

]a,c,e

2.2.2 Loading Conditions

Thermal Transient Selection for Maximum Allowable Flaw Size Determination

The requirement for evaluation of a flaw using the rules of Section XI is that the governing transients be chosen from the normal/upset conditions as well as from the emergency/faulted conditions. This is necessary because, as discussed in Section 2.1, different safety margins are used for the normal/upset conditions and the emergency/faulted conditions. Lower safety factor is used to reflect the lower probability of occurrence for the emergency/faulted conditions.

[

]a,c,e

Thermal Transient Selection for Fatigue Crack Growth Prediction

[

]a,c,e The thermal transients that occur in the upper head region are relatively mild, because most of the water in the head region has already passed through the core region. The flow in the upper head region is low compared to other regions of the reactor vessel, which mutes the effects of the operating thermal transients. The thermal transients that occur in Beaver Valley Unit 2 are shown in Table 2-1. [

]a,c,e

Since Beaver Valley Unit 2 is operated as a base-load plant, and does not change power to respond to the demands of the grid. The cycles for the unit loading and unloading transient were reduced from 18300 to 4000, based on conservative operating plant experience for base-load plants.

2.2.3 Stress Intensity Factors

One of the key elements in a fracture mechanics evaluation is the determination of the crack driving force or stress intensity factor (K_I). This is based on the equations available in the literature.

Stress Intensity Factor for Surface Flaw

For a part-through wall flaw, the stress profile is approximated by a cubic polynomial as follows:

$$\sigma(x) = A_0 + A_1 x + A_2 x^2 + A_3 x^3$$

where:

x = The distance into the wall (inch)
σ = Stress perpendicular to the plane of the crack (ksi)
A_i = Coefficients of the cubic polynomial Fit, i = 0, 1, 2, 3

[

]^{a,c,e}

2.2.4 Allowable Flaw Size Determination

Allowable flaw sizes for axial and circumferential flaws with various aspect ratios (flaw length/flaw depth) in a CRDM penetration nozzle are calculated in accordance with the acceptance criteria discussed in Section 2.1. The thermal transients that have the [ ]^{a,c,e} were considered in determining the allowable flaw sizes. It should be noted that these allowable flaw sizes must be adjusted to account for fatigue crack growth. Since the repaired flaws are embedded and sealed, they are not subjected to PWSCC. Adjustments to the allowable flaw sizes are based on the results from the fatigue crack growth evaluation described in Section 2.2.5.

2.2.5 Fatigue Crack Growth Prediction

The analysis procedure involves postulating various type of flaws in the penetration nozzle subjected a series of design loads. The applied loads include pressure, thermal transient and residual stresses. The governing thermal transients used for this evaluation are shown in Section 2.2.2. The cycles are distributed evenly over the entire plant design life. The stress intensity factor range, ΔK_I, that controls fatigue crack growth, depends on the geometry of the crack, its surrounding structure and the range of applied stresses in the region of the postulated crack. Once ΔK_I is calculated, the fatigue crack growth due to a particular stress cycle can be determined using a crack growth rate reference curve applicable to the material of the head penetration nozzle.

The crack growth rate (CGR) reference curves for these nickel base alloys have not been developed for Section XI in the Code, therefore information available from the literature was used. [

]a,c,e

The crack growth rate reference curve in air for the repair weld Alloy 52 is not available. There are 4 tests on Alloy 52 in PWR water environment. The available data in reference 9 showed Alloy 52 and Alloy 600 have the same CGR in PWR Water environment. Therefore, Alloy 600 CGR in air could be used as Alloy 52 CGR in air.

Once the incremental crack growth corresponding to a specific transient, for a small time period, is calculated, it is added to the original crack size, and the analysis continues to the next time period and/or thermal transient. The procedure is repeated in this manner until all the significant analytical thermal transients and cycles known to occur in a given period of operation have been analyzed.

2.3 FRACTURE MECHANICS ANALYSIS RESULTS

Axial and circumferential flaws found on the inside surface of a CRDM head penetration nozzle can be repaired using the embedded flaw repair method. A range of potential flaw sizes and shapes was investigated to thoroughly evaluate the embedded flaw repair method.

2.3.1 Results for Allowable Flaw Sizes (Without Fatigue Crack Growth Adjustment)

Allowable Flaw Sizes for Axial Flaws

[

]a,c,e

The allowable flaw sizes for a maximum design pressure of 2.5 ksi can then be determined as shown in Figure 2-3 for a postulated inside surface axial flaw with a given aspect ratio (flaw length/flaw depth). It should be noted that the allowable flaw sizes determined this way for the inside surface axial flaws can be [ ]^{a,c,e} Allowable flaw sizes determined from Figure 2-3 must be adjusted to account for the fatigue crack growth of the repaired flaws, which are embedded and free from stress corrosion cracking. The amount of adjustments is described in Section 2.3.2.

Allowable Flaw Sizes for Circumferential Flaws

[

]^{a,c,e} The allowable flaw sizes for a maximum design pressure of 2.5 ksi can then be determined as shown in Figure 2-4 for a postulated inside surface circumferential flaw with a given aspect ratio (flaw length/flaw depth). It should be noted that the allowable flaw sizes determined this way for the surface flaws can be [ ]^{a,c,e} Allowable flaw sizes determined from Figure 2-4 must be adjusted to account for the fatigue crack growth of the repaired flaws, which are embedded and free from stress corrosion cracking. The amount of adjustments is described in Section 2.3.2.

2.3.2 Results for Allowable Flaw Sizes (With Fatigue Crack Growth Adjustment)

Fatigue crack growth evaluation was performed to determine the potential crack growth for the outside surface flaws. The FCG results for the outside surface flaws envelop those for the embedded flaws of comparable sizes. Therefore, the FCG results can be applied to both outside surface flaws and embedded flaws.

Allowable Axial Flaw Sizes

Figures 2-5 and 2-6 show the fatigue crack growth prediction of the CRDM penetration nozzles for a range of flaw depths at uphill side and downhill side, respectively. It should be noted that the total flaw depth is limited to 75% of the wall thickness in all cases except for the flaws with aspect ratio (flaw length/flaw depth) of 10. The allowable flaw depth for longer flaw with aspect ratio of 10 is 74% of the wall thickness. The allowable flaw sizes could be determined from these figures, by subtracting the fatigue crack growth increments from the ASME Code allowable flaw sizes shown on Figure 2-3, for the desired period of service life. For example, Figure 2-7 shows the allowable flaw sizes for 10 years period of service life.

Allowable Circumferential Flaw Sizes

Figures 2-8 and 2-9 show the fatigue crack growth prediction of the CRDM penetration nozzles for a range of flaw depths at uphill side and downhill side, respectively. It should be noted that the total flaw depth is limited to 75% of the wall thickness in all cases. The initial allowable flaw sizes could be determined from these figures, by subtracting the fatigue crack growth increments from the ASME Code

allowable flaw sizes shown on Figure 2-4, for the desired period of service life. For example, Figure 2-10 shows the allowable flaw sizes for 10 years period of service life.

2.4 SUMMARY

Axial and circumferential flaws found on the inside surface or outside surface of a CRDM head penetration nozzle can be repaired using the embedded flaw repair method to seal it from the primary water environment. The maximum allowable axial and circumferential flaw sizes in the repaired penetration nozzles are shown in Figures 2-7 and 2-10 with the effects of fatigue crack growth included. For other period of service life, the maximum allowable flaw sizes can be determined from Figures 2-3 and 2-4 with the aid of 2-5, 2-6, 2-8 and 2-9.

Table 2-1 Summary of Reactor Vessel Transients for Beaver Valley Unit 2 [2, 3]

Normal Conditions	**Number of Occurrences**
Plant Heatup And Cooldown	200
Load Follow Cycles (Unit Loading And Unloading At 5% /Minute)	18300*
Step Load Increase And Decrease (10% Of Full Power)	2,000
Large Step Load Decrease With Steam Dump	200
Refueling	80
Steady State Fluctuations	Infinite
Upset Conditions	
Loss of load w/o Immediate Turbine or Reactor Trip	80
Loss of Power	40
Loss of Flow	80
Reactor Trip From Full Power	400
Inadvertent Auxiliary Spray	10
Inadvertent Safety Injection	60
RCS Cold Depressurization	10
Operating Basis Earthquake (OBE)	400
Test Conditions	
Turbine Roll Test	10
Primary Side Hydrostatic Test	5
Secondary Side Hydrostatic Test	5
Primary Side Leak Test	50
Emergency Faulted Conditions	
Main Reactor Coolant Pipe Break	1
Steam Pipe Break	1
Steam Generator Tube Rupture	1
Design Basis Earthquake	1

* 4000 cycles were used since Beaver Valley Unit 2 is a base-load plant

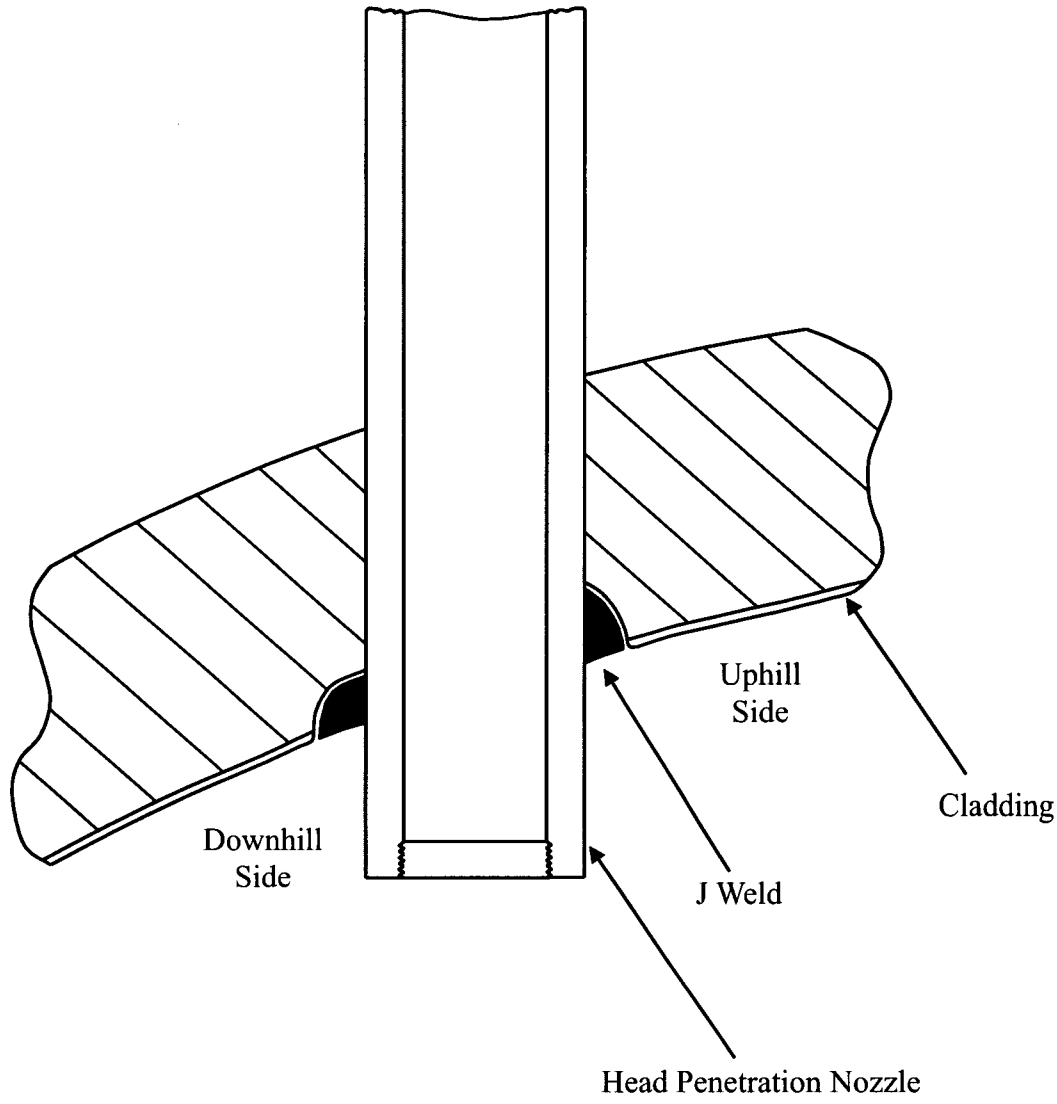

Figure 2-1 Geometry of Closure Head Penetration for a Typical Westinghouse Design

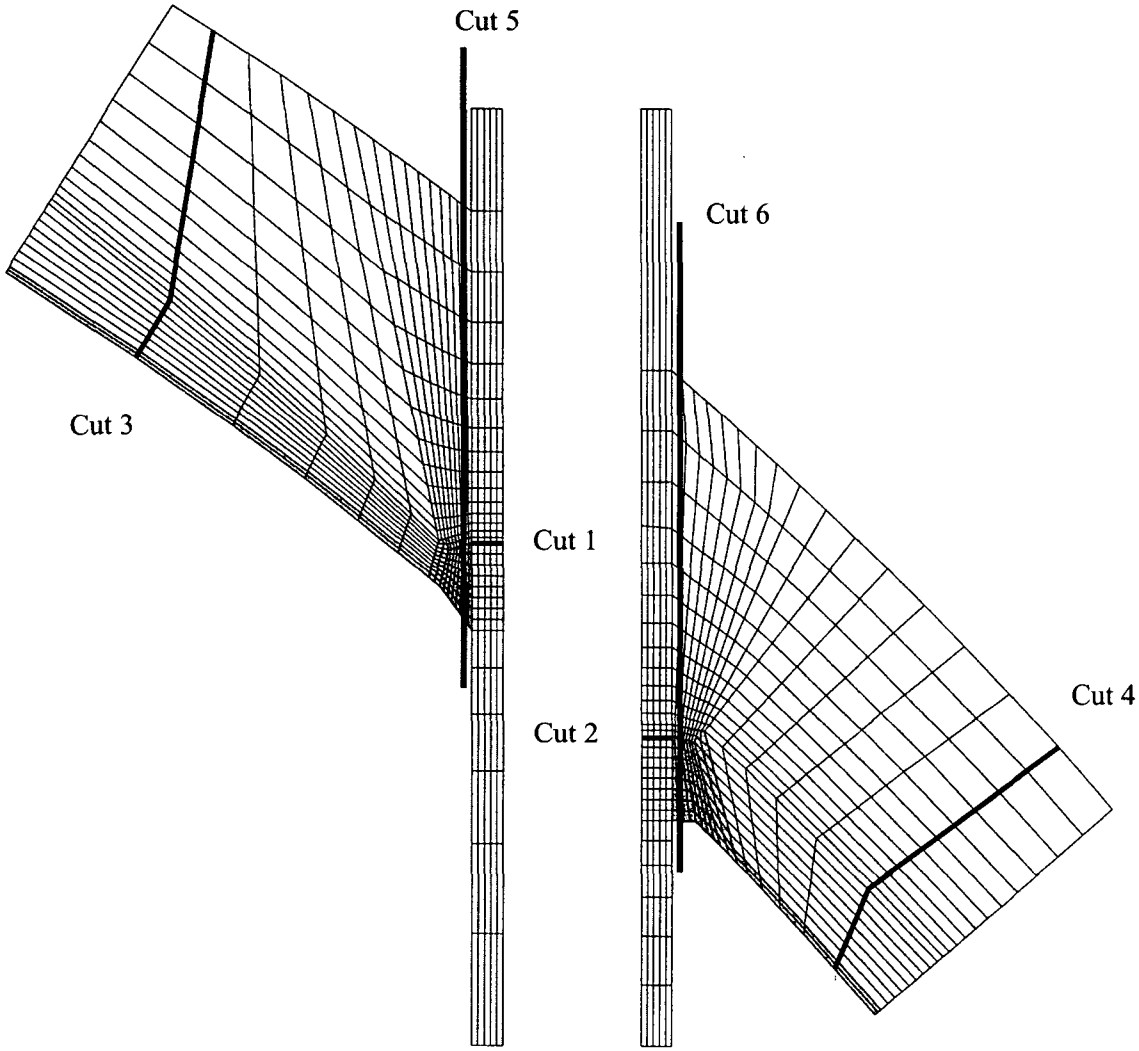

Figure 2-2 Finite Element Model with Analytical Stress Cuts Identified

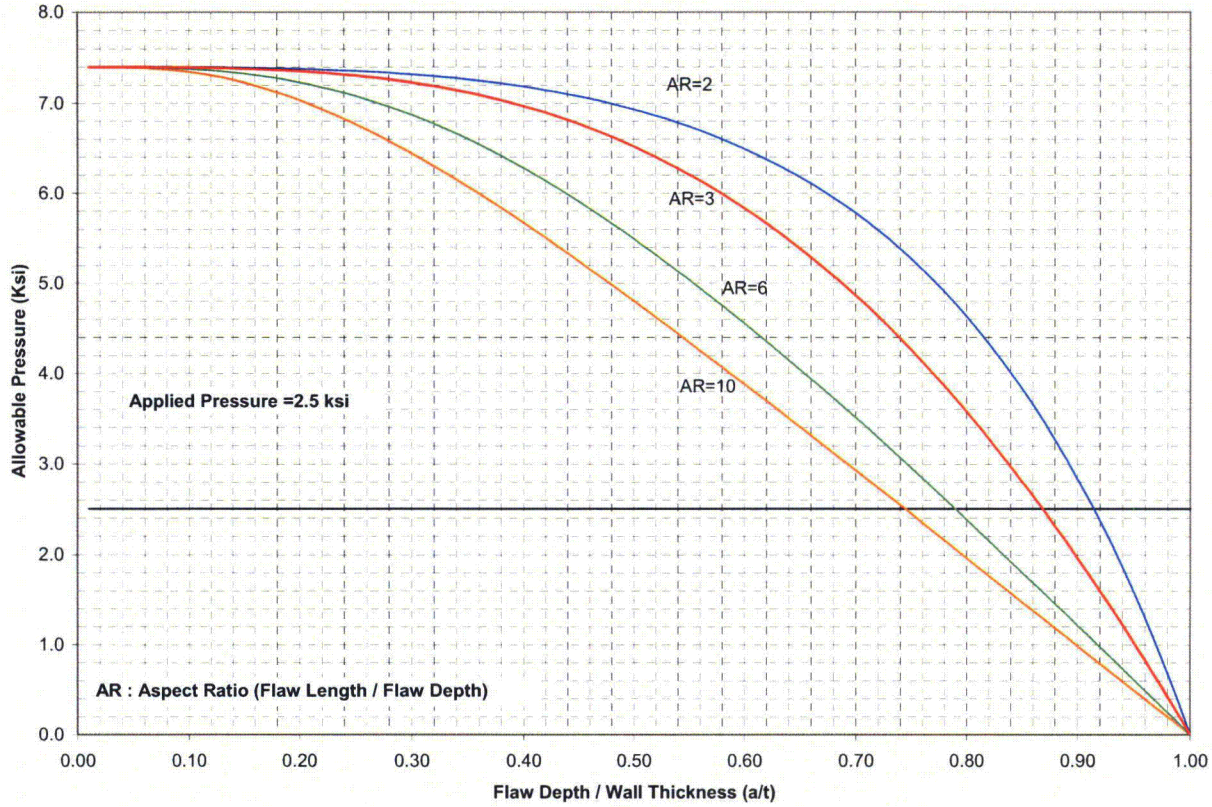

Figure 2-3 Allowable Embedded Axial Flaw Sizes In CRDM Penetration Nozzle (Without Fatigue Crack Growth) [ ]^{a,c,e}

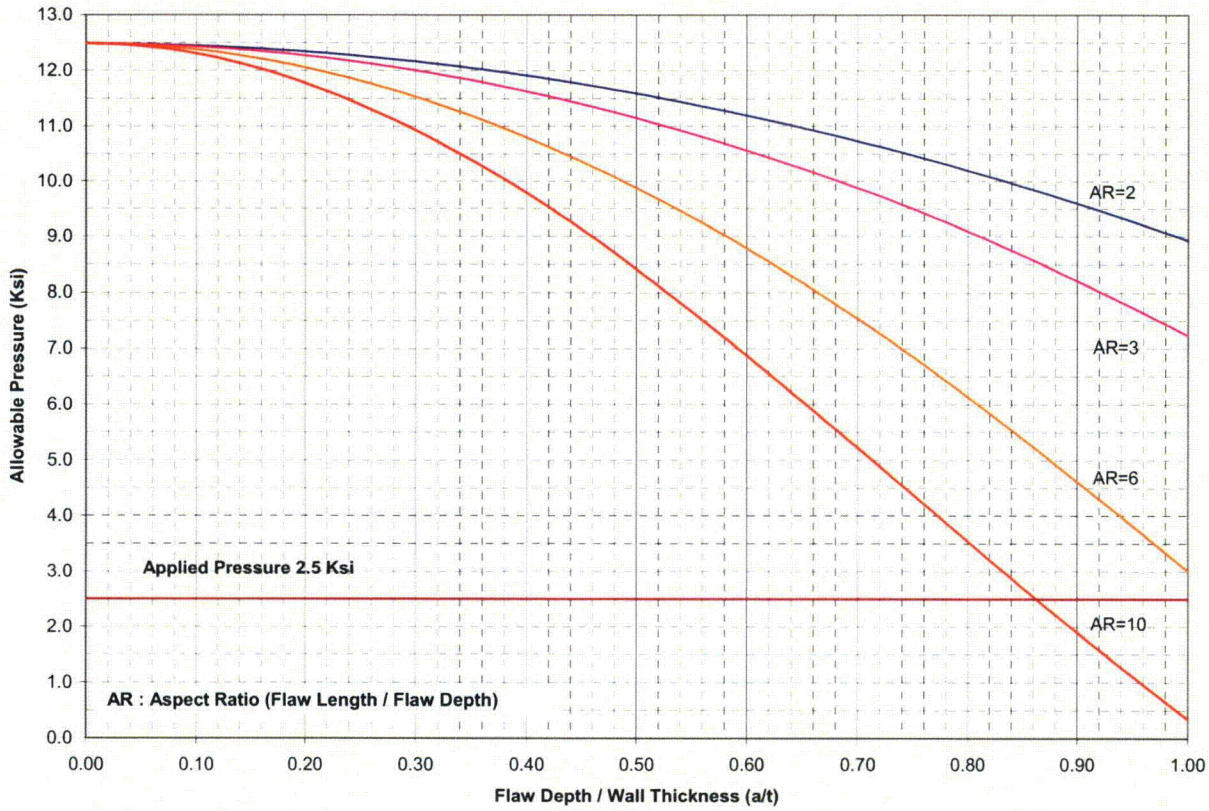

Figure 2-4 Allowable Embedded Circumferential Flaw Sizes In CRDM Penetration Nozzle (Without Fatigue Crack Growth) [ ]^{a,c,e}

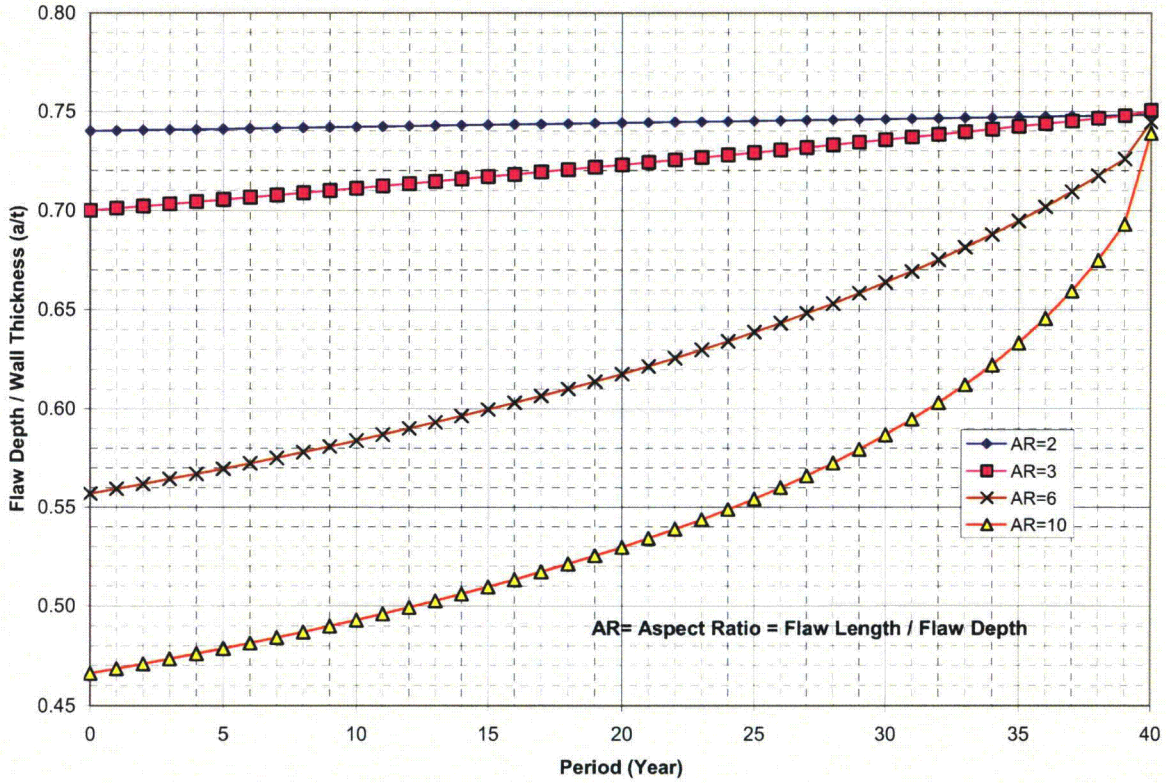

Figure 2-5 Fatigue Crack Growth Prediction for Repaired Axial Flaws in the CRDM Penetration Nozzles (Uphill side)

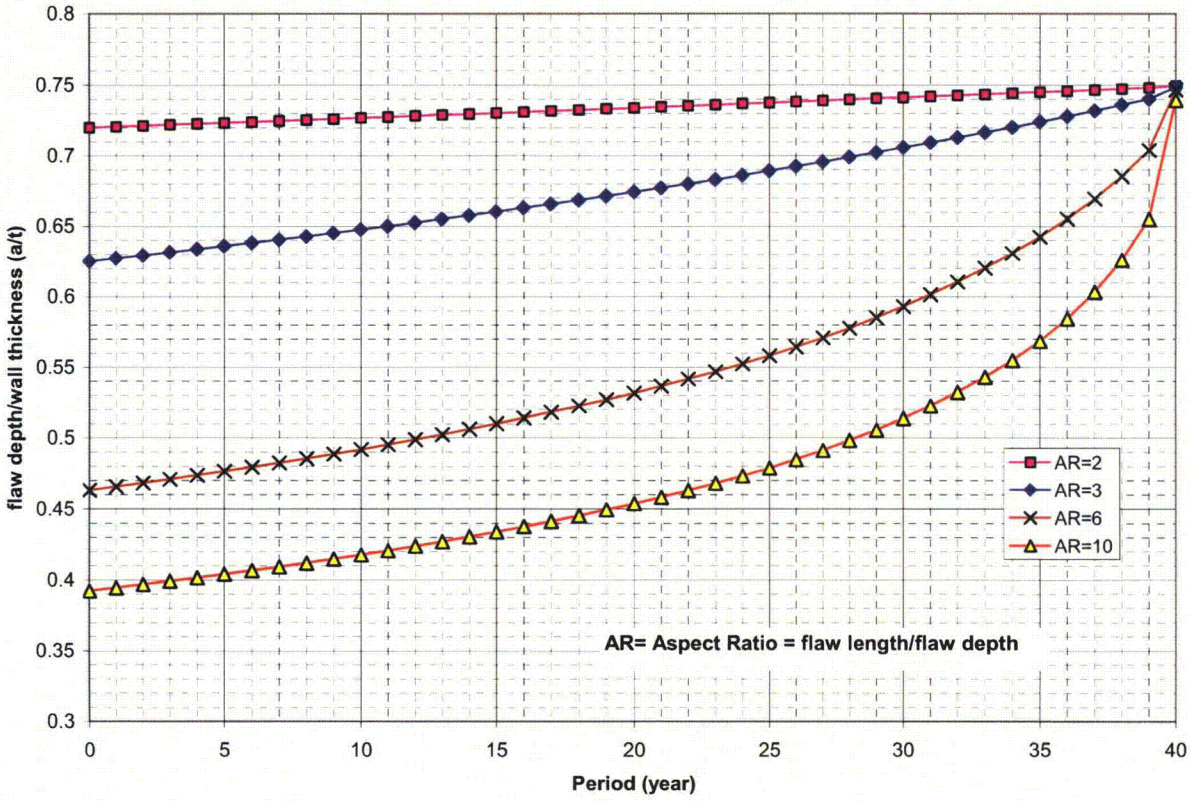

Figure 2-6 Fatigue Crack Growth Prediction for Repaired Axial Flaws in the CRDM Penetration Nozzles (Downhill side)

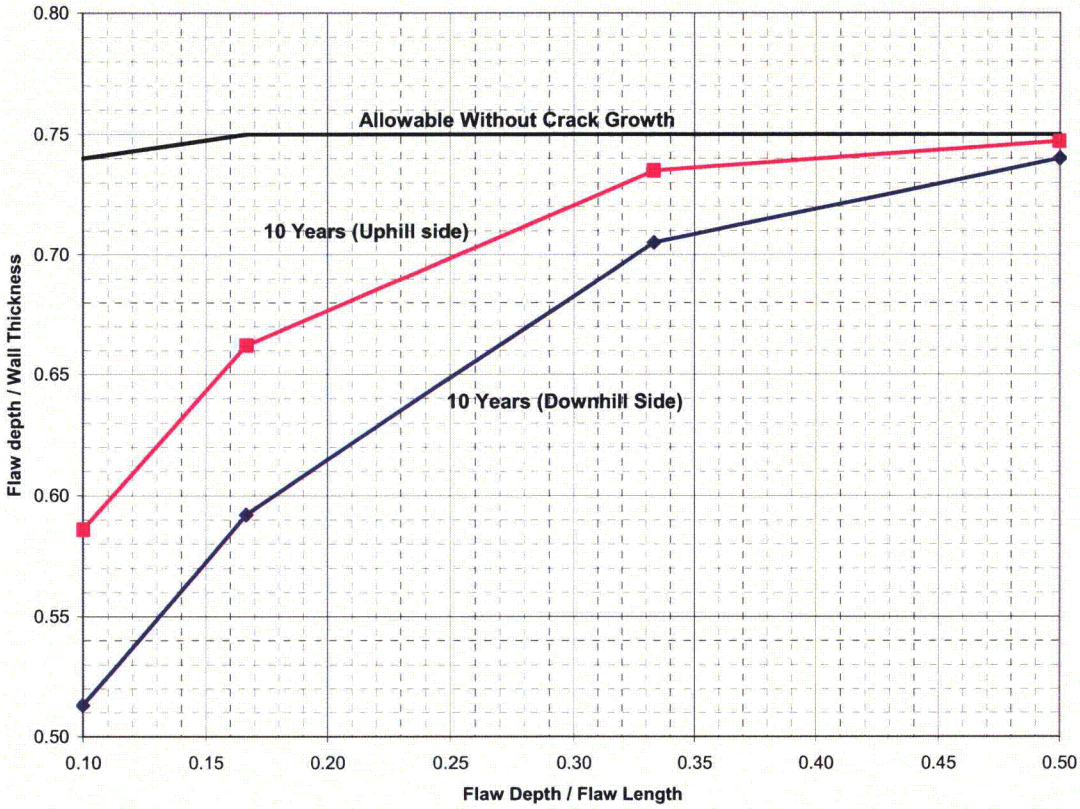

Figure 2-7 Maximum Allowable Axial Flaw Sizes in the CRDM Penetration Nozzles for 10 years Service Life

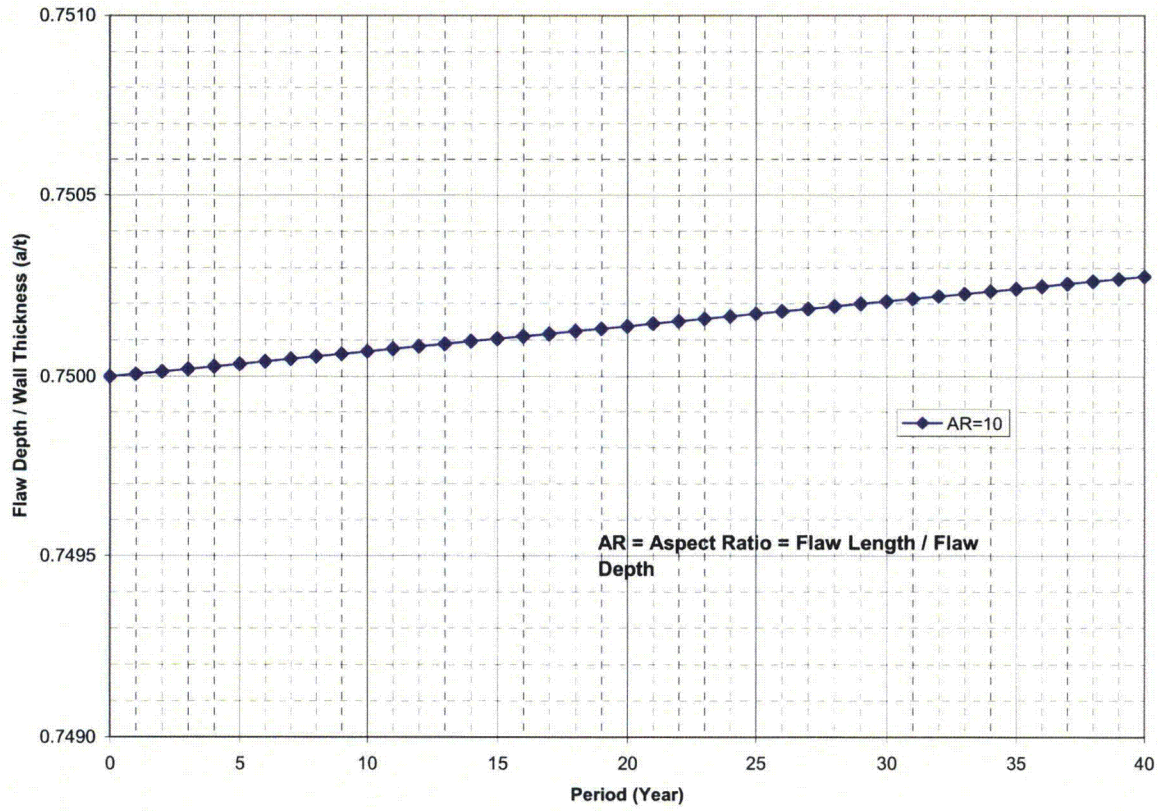

Figure 2-8 Fatigue Crack Growth Prediction for Circumferential Flaws in the CRDM Penetration Nozzles (Uphill side)

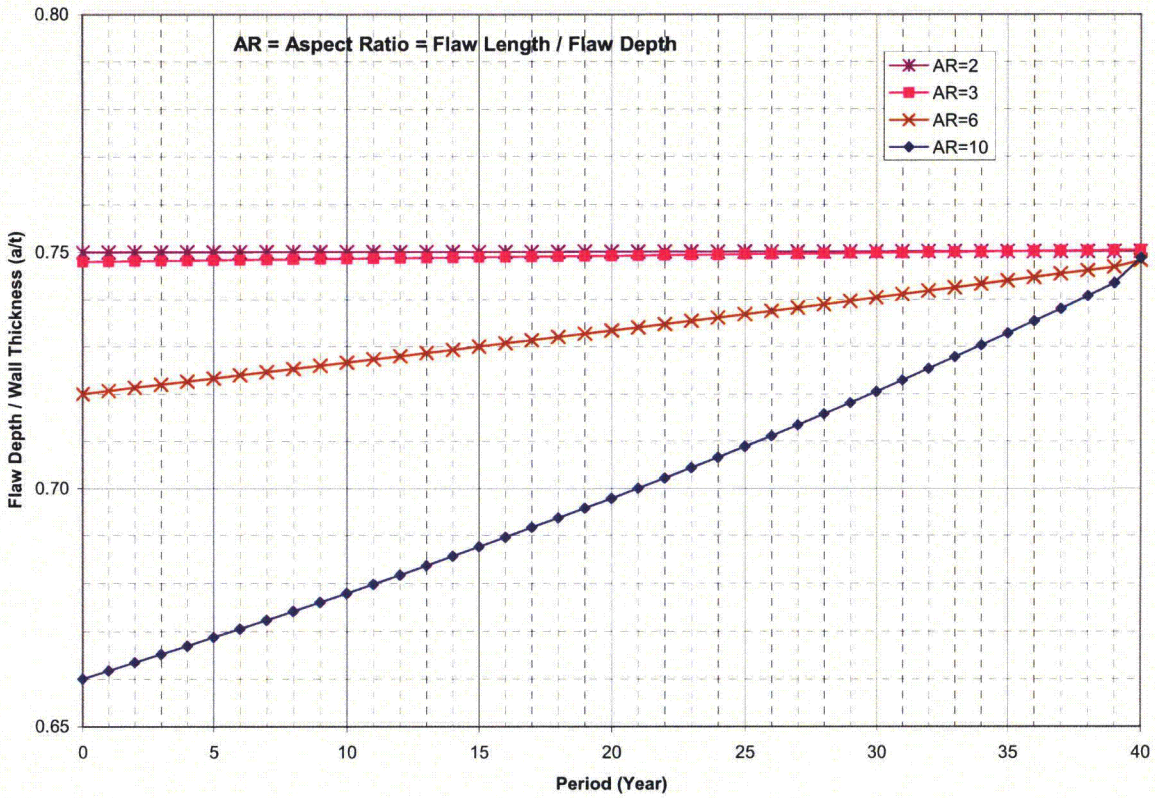

Figure 2-9 Fatigue Crack Growth Prediction for Circumferential Flaws in the CRDM Penetration Nozzles (Downhill side)

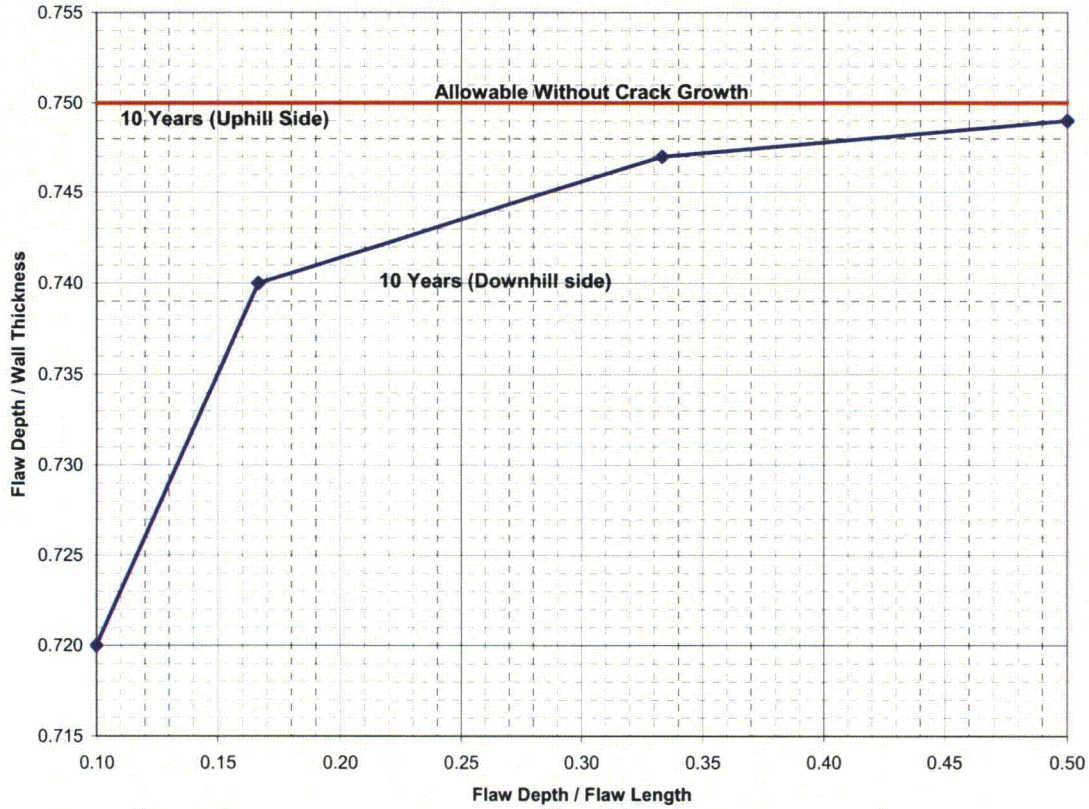

Figure 2-10 Maximum Allowable Circumferential Flaw Sizes in the CRDM Penetration Nozzles for 10 years Service Life

3 TECHNICAL BASIS FOR APPLICATION OF EMBEDDED FLAW REPAIR TECHNIQUE TO PENETRATION NOZZLE ATTACHMENT WELDS

This section provides a discussion on the technical basis for the use of embedded flaw repair method for a flawed head penetration attachment weld. [

]^{a,c,e} A flaw evaluation was carried out by postulating a planar flaw in the reactor vessel head of that size. [

]^{a,c,e}

3.1 Acceptance Criteria

3.1.1 Section XI Appendix K

The acceptance criteria and evaluation procedures used to demonstrate structural integrity of the reactor vessel closure head is Appendix K of ASME Code Section XI [1]. Although the original purpose of Appendix K was evaluation of reactor vessels with low upper shelf fracture toughness, the methods are equally applicable to any region of the reactor vessel where the fracture toughness can be described with elastic plastic parameters. The head region of the reactor vessel is one of the hottest portion of the reactor vessel where the steady state temperature is approximately 550-620 °F. This ensures ductile behavior, and so the use of elastic-plastic methods is appropriate.

This approach to the integrity of a nuclear vessel has been developed over a ten-year period, and has been illustrated with a number of example problems [15] to demonstrate its use. The extension of this methodology to issues other than the low shelf fracture toughness issue is appropriate when service conditions (temperature) ensure ductile behavior. The extension of the Elastic Plastic Fracture Mechanics (EPFM) method to the reactor vessel head is appropriate, as discussed above.

The acceptance criteria are to be satisfied for each category of transients, namely, Service Load Levels A and B (normal and upset), Level C (emergency) and Level D (faulted) conditions. The criteria are listed below:

$$J < J_{0.1}$$

$$\frac{\partial J}{\partial a} < \frac{dJ_R}{da}$$

J_R = J-integral resistance to ductile tearing for the material

J = Applied J-integral, enlarged by a safety factor of 1.15

$J_{0.1}$ = J-integral resistance at a ductile flaw extension of 0.1 inch

$\frac{\partial J}{\partial a}$ = Partial derivative of the applied J-integral with respect to flaw depth, a

$\frac{dJ_R}{da}$ = Slope of the J-R curve

3.1.2 Primary Stress Limits

In addition to satisfying the Section XI criteria, the primary stress limits of paragraph NB 3000 in Section III of the ASME Code must be satisfied. The effects of a local area reduction that is equivalent to the area of the postulated flaw in the vessel head attachment weld must be considered by increasing the membrane stresses to reflect the reduced cross section. The primary hydro test condition is the governing case for this limit, since it has the pressure loading of 3125 psia. The allowable flaw depth was determined by evaluating the primary stress of spherical head with reduced wall thickness. The results show the allowable flaw depth is much bigger than the weld size.

3.2 METHODOLOGY

The evaluation assumed that a flaw has been detected in a penetration nozzle attachment weld and that the embedded flaw repair method is used to seal the flaw from further exposure to the primary water environment. The evaluation demonstrated the flaw is stable under ductile crack growth based on the acceptance criteria described in Section 3.1, for a postulated flaw in the vessel head near the penetration nozzle that encompassed the entire attachment weld region. [

]^{a,c,e} Therefore, the fatigue crack growth evaluations for the reactor vessel head and the repair welds were performed to ensure the structural integrity.

3.2.1 Geometry and Source of Data

There are many head penetrations in the reactor vessel upper head, and [

]^{a,c,e} The distribution of residual, transient thermal, and pressure stresses in the closure head region is obtained from detailed three-dimensional elastic-plastic finite element analyses of the head penetration nozzle region using iso-parametric finite elements [14]. [

]^{a,c,e} [

]^{a,c,e} The through-wall stress distributions from the finite element analyses were used to determine the maximum allowable flaw sizes and to predict fatigue crack growth for the postulated flaws in the attachment weld regions. Two stress cuts were selected for the analysis and the finite element model with the selected stress cuts is shown in Figure 2-2. Stress cut 5 is on the uphill side of the outermost penetration nozzle and stress cut 6 is on the downhill side.

3.2.2 Loading Conditions

Thermal Transient Selection for Maximum Allowable Flaw Size Determination

The requirement for an evaluation of a flaw using the rules of Section XI is that the governing transients be chosen for the normal/upset conditions as well as the emergency/faulted conditions. The governing transient for determining the flaw stability under ductile crack growth is determined to be the unit loading and unloading transient, which results in the highest stress intensity factor.

Thermal Transient Selection for Fatigue Crack Growth Prediction

[ ]^{a,c,e} The thermal transients that occur in the upper head region are relatively mild because most of the water in the head region has already passed through the core region. The flow in the upper head region is low compared to other regions of the reactor vessel, which mutes the effects of the operating thermal transients. The thermal transients that occur in Beaver Valley Unit 2 are shown in Table 2-1. [

]^{a,c,e}

Since Beaver Valley Unit 2 is operated as a base-load plant, and does not change power to respond to the demands of the grid. The cycles for the unit loading and unloading transient were reduced from 18300 to 4000, based on conservative operating plant experience for base-load plants.

3.2.3 Stress Intensity Factor Calculation

One of the key elements in a fracture mechanics evaluation is the determination of the crack driving force or stress intensity factor (K_I). This is based on the information available in the literature.

The stress intensity factors for two corner flaws emanating from the edge of a hole in a plate was taken from the data by [ ]^{a,c,e} Use of this method requires that the stresses remote from the hole be resolved into membrane and bending stress components. The stress intensity factor can be expressed conservatively in terms of the membrane and bending stress components as follows:

[

]^{a,c,e} This flexibility is necessary because this expression will be applied to a range of flaw shapes corresponding to different attachment weld shapes in Beaver Valley Unit 2. The coefficients A and B can be found in [ ]^{a,c,e} for selected values of r/t, a/l and a/t, where "r" is the outside radius of the penetration nozzle and "t" is the wall thickness of the reactor vessel head. For the r/t, a/l and a/t values that are not shown in [ ]^{a,c,e}, the coefficients A and B were determined using interpolation. Since the coefficients are provided for various locations around the flaw front, [

]^{a,c,e}

The stress intensity factors for the resulting embedded flaws due to the embedded flaw repair method were calculated based on the method of Appendix A of Section XI. The sub-surface stress intensity factors expression can apply to the crack approaching the surface of the component as stated in the technical basis [11]. The stress intensity factor can be expressed in terms of the equivalent membrane and bending stress components as follows:

$$K_I = \left(\sigma_m M_m + \sigma_b M_b\right)\sqrt{\pi a / Q}$$

where

σ_m, σ_b = Equivalent membrane and bending stresses, as defined in A-3200(a) of Code [1]. (See Figure 3-4 (a))

M_m, M_b = Correction factors for the membrane and bending stresses. The equations for the correction factors are listed in Reference 11

a = One-half the axis of elliptical flaw

Q = Flaw shape parameter as defined in Reference 11

3.2.4 Material Properties

One of the most important information on the toughness for pressure vessel and piping materials is the J-R curve, or JR-curve, of the material, where JR stands for material resistance to crack extension, as represented by the measured J-integral value versus crack extension. Simply put, J-R curve to cracking resistance is as significant as the stress-strain curve to load-carrying capacity and ductility of a material. Both J-R curve and stress-strain curve are properties of a material.

Unfortunately, directly measured JR-curves are not generally available for a specific material of interest. Fortunately, methods that can generate such information from available data such as material chemistry, radiation exposure, temperature and Charpy V-notch energy, is now available [15]. The method provided in Reference 15 summarizes a large collection of public test data, and fitted into multivariable model

based on advanced pattern recognition technology. Separate analysis models and databases were developed for different material groups, including reactor pressure vessel (RPV) welds, RPV base metals, piping welds, piping base metals and a combined materials group.

The material resistance J-values, J_{mat}, are fitted into the following equation [4, 15]:

$$J_{mat} = (MF)C1\,(\Delta a)^{C2} \exp\,[C3(\Delta a)^{C4}]$$

where C1, C2, C3, and C4 are fitting constants, and Δa is crack extension.
MF is the Margin Factor from Reference 4:
MF= 0.749 for Service Levels A, B and C
MF= 1.0 for Service Level D

For the RPV base metal model, the constants C1, C2, C3, and C4 are taken from Table 11 of Reference 15. C1, C2, C3, and C4 are complicated parameters as defined below:

$$\ln C1 = a_1 + a_2 \ln CVNp + a_3 T + a_4 \ln B_n + a_5 \phi t$$
$$C2 = d_1 + d_2 \ln C1 + d_3 \ln B_n$$
$$C3 = d_4 + d_5 \ln C1 + d_6 \ln B_n$$
$$C4 = d_7$$

where T = Temperature (°F),
B_n = Section thickness (inches).
CVNp = Charpy impact energy (ft-lbs) = 137 ft-lb from Certified Material Test Report [6].
ϕt = Fluence ($x10^{18}$ n/cm^2, E>1Mev).

a_1, a_2, a_3, a_4, a_5, d_1, d_2, d_3, d_4, d_5, d_6, d_7 (briefly, a_i and d_i) are constants given in Table 11 of Reference 15:

$a_1 = -2.44$

$a_2 = 1.13$

$a_3 = -0.00277$

$a_4 = 0.0801$

$d_1 = 0.0770$

$d_2 = 0.116$

$d_3 = -0.0412$

$d_4 = -0.0812$

$d_5 = -0.00920$

$d_6 = -0.0295$

$d_7 = -0.409$

Neutron irradiation has been shown to produce embrittlement that reduces the toughness properties of reactor vessel ferritic steel material. The irradiation levels are very low in the reactor vessel head region and therefore the fracture toughness will not be measurably affected.

3.2.5 Applied J-Integral

For small scale yielding, $J_{applied}$ of a crack can be calculated by the Linear Elastic Fracture Mechanics (LEFM) method. A plastic zone correction must be performed to account for the plastic deformation at the crack tip. The plastic deformation ahead of the crack front is then regarded as a failed zone and the crack size is, in effect, increased. The K_I-values can be converted to $J_{applied}$ by the following equation:

$$J_{applied} = \frac{K_{ep}^2}{E'}$$

where K_{ep} is the elastically calculated K_I-value based on the plastic zone adjusted crack depth or size
$E' = E/(1-\nu^2)$ for plane strain, $E' = E$ for plane stress, E = Young's Modulus,
and ν = Poisson's Ratio.

The plastic zone size, r_p, is calculated by

$$r_p = \frac{1}{6\pi}\left(\frac{K_I}{S_y}\right)^2$$

where S_y is the yield strength of the material. Assume that the crack depth is a_o, the K_{ep} can now be calculated based on a new crack length, $a_o + r_p$. For small scale yielding, K_{ep} can be simplified as follows:

$$K_{ep} = f\ K_I$$

Where

$$f = \sqrt{\frac{(a_0 + r_P)}{a_0}}$$

3.2.6 Fatigue Crack Growth Prediction

The analysis procedure involves postulating planar flaws that extend radially over the entire attachment weld cross-section in the penetration and are subjected to a series of design loads. The loading included pressure, thermal transients, and residual stresses. The transients used for this evaluation are shown in Section 3.2.2 and the cycles are distributed evenly over the plant design life. The stress intensity factor range, ΔK_I, which controls the fatigue crack growth, depends on the geometry of the crack, its surrounding structure and the range of applied stresses in the region of the postulated crack. Once ΔK_I is

calculated, the fatigue crack growth due to a particular stress cycle can be determined using a crack growth rate reference curve applicable to the material where the crack is postulated.

The crack growth rate curves used in the analyses for the postulated flaws in the reactor vessel head are taken directly from [ ]^{a,c,e} Since the flaw is sealed from the primary water environment, the crack growth rate reference curve for the air environment is used. This curve is a function of the applied stress intensity factor range (ΔK_I) and the R ratio, which is the ratio of the minimum to maximum stress intensity factor during a thermal transient. [

]^{a,c,e}

Once the incremental crack growth corresponding to a specific transient, for a small time period, is calculated, it is added to the original crack size, and the analysis continues to the next time period and/or thermal transient. The procedure is repeated in this manner until all the significant analytical thermal transients and cycles known to occur in a given period of operation have been analyzed.

3.3 FRACTURE MECHANICS ANALYSIS RESULTS

3.3.1 Results for Applied J-Integral and J-R Curve

The actual geometry or weld shapes of Beaver Valley Unit 2 head penetration attachment welds [7, 13] are shown in Table 3-1, which forms the basis for the geometry of the postulated flaws in the attachment weld region. The stress intensity factors were calculated for the biggest weld sizes, penetration 58-65 downhill side welds, that were selected to bound all the other penetration nozzle attachment weld shapes in Beaver Valley Unit 2.

The applied J-integral values were evaluated based on the method describe in Section 3.2. The material J-R Curve was obtained by setting the Margin Factor (MF) to 0.749. The applied J-integral values and material J-R Curve were tabulated in Table 3-2 and plotted in Figure 3-2.

The key aspect of the analysis is the slope of the J-material curve and the slope of the J-applied curve. Figure 3-2 demonstrated that the flaw is stable with the slope of the J-material curve far exceeds the slope of the J-applied curve and $J_{applied} < J_{0.1}$. Therefore, all the head penetration welds have been shown to be acceptable to the code requirement.

3.3.2 Results for Fatigue Crack Growth

The fatigue crack growth was determined for the worst case (downhill of penetrations 58-65) which envelops all other attachment welds in Beaver Valley Unit 2. As shown in Figure 3-3 for the downhill side weld, the predicted crack growth for the head penetration attachment welds due to fatigue is not significant.

3.3.3 Fatigue Crack Growth into the Repair Weld

[

]^{a,c,e}

The predicted fatigue crack growth for the postulated weld shapes is shown in Table 3-3. The FCG prediction results indicate that the repaired weld can last at least 5 years of service life depending on the initial flaw depth. These weld shapes cover all other weld shapes in the penetration nozzle attachment welds for Beaver Valley Unit 2.

3.4 SUMMARY

The results of the evaluation have demonstrated that the embedded flaw repair method is a viable method for repairing flaws found in the J-weld. The repaired J-weld would last at least 5 years of service life regardless of the size of the flaw in the penetration nozzle attachment weld.

Table 3-1 Geometry of Beaver Valley Unit 2 Head Penetration Attachment Welds (All dimensions in inches)

	Uphill				Downhill		
Pen #	l	a	a/l		l	a	a/l
1	0.88	0.97	1.10		0.88	0.97	1.10
2-5	0.88	1.07	1.22		0.94	0.97	1.03
6-9	0.89	1.12	1.26		0.99	0.99	1.00
10-13	0.91	1.19	1.31		1.04	1.01	0.97
14-17	0.91	1.21	1.33		1.06	0.99	0.93
18-21	0.94	1.29	1.37		1.16	1.01	0.87
22-25	0.95	1.31	1.38		1.20	1.02	0.85
26-33	0.96	1.33	1.39		1.23	1.02	0.83
34-41	1.00	1.41	1.41		1.35	1.02	0.76
42-45	1.04	1.48	1.42		1.49	1.04	0.70
46-53	1.06	1.46	1.38		1.56	1.05	0.67
54-57	1.08	1.53	1.42		1.61	1.06	0.66
58-65	1.12	1.61	1.44		1.77	1.07	0.60

Note : The values a (weld depth) and l (weld length) are dimensions of the J-weld only and do not include the dimensions of the fillet weld

Table 3-2 Results of Applied J-integral and Material J-R Curve

a (inch)	J_{mat} (kip-in/in^2)	$J_{applied}$ (kip-in/in^2)
1.074	0.303	1.290
1.078	0.485	1.295
1.082	0.613	1.300
1.086	0.712	1.304
1.090	0.793	1.309
1.094	0.863	1.314
1.098	0.924	1.319
1.102	0.978	1.324
1.106	1.027	1.329
1.110	1.072	1.333
1.114	1.113	1.338
1.118	1.151	1.343
1.122	1.186	1.348
1.126	1.219	1.353
1.130	1.250	1.357
1.134	1.280	1.362
1.138	1.308	1.367
1.142	1.334	1.372
1.146	1.360	1.377
1.150	1.384	1.381
1.154	1.407	1.386
1.158	1.429	1.391
1.162	1.451	1.396
1.166	1.471	1.401
1.170	1.491	1.405

Table 3-3 Results of Fatigue Crack Growth Analysis for the Repaired Attachment Welds

	Downhill Side		Uphill Side	
Year	X1 (inch)	X2 (inch)	X1 (inch)	X2 (inch)
0	0.156	1.516	0.156	1.996
1	0.154	1.518	0.140	2.000
2	0.151	1.519	0.122	2.003
3	0.149	1.521	0.101	2.007
4	0.146	1.523	0.075	2.010
5	0.144	1.525	0.038	2.014

Note:

X1 = distance from the free surface for point 1.

X2 = distance from the free surface for point 2.

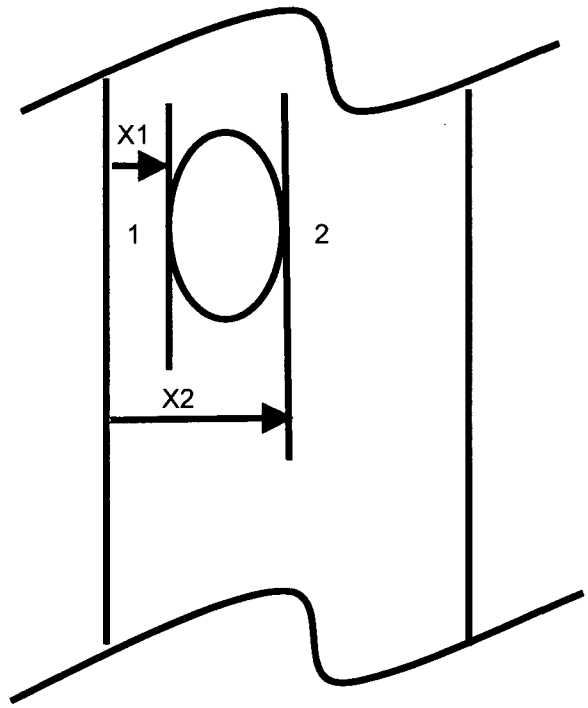

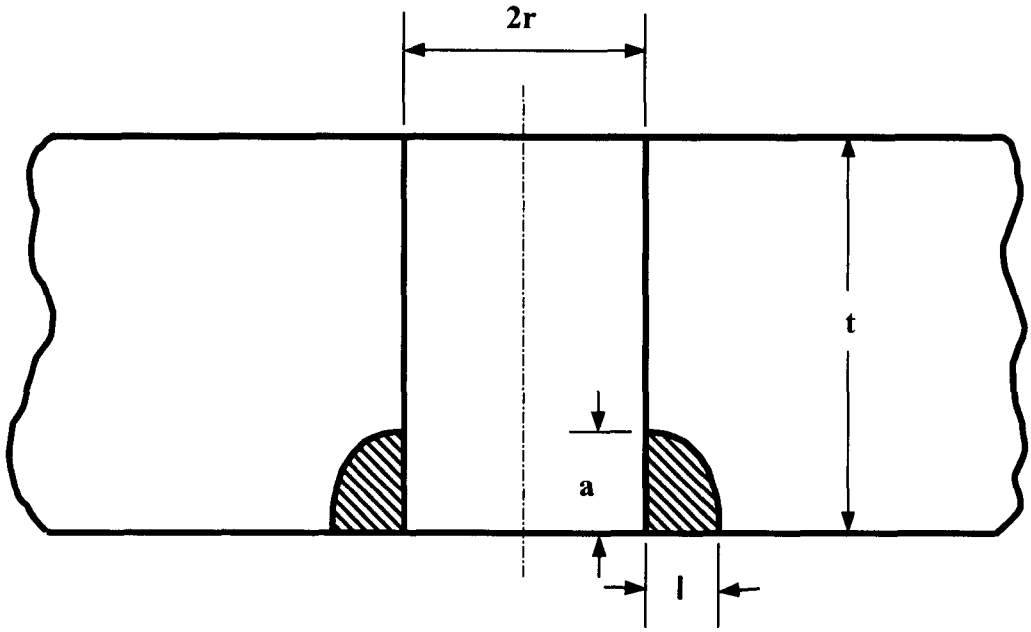

Figure 3-1 Geometry and Terminology as Applied in [ ]^{a,c,e}

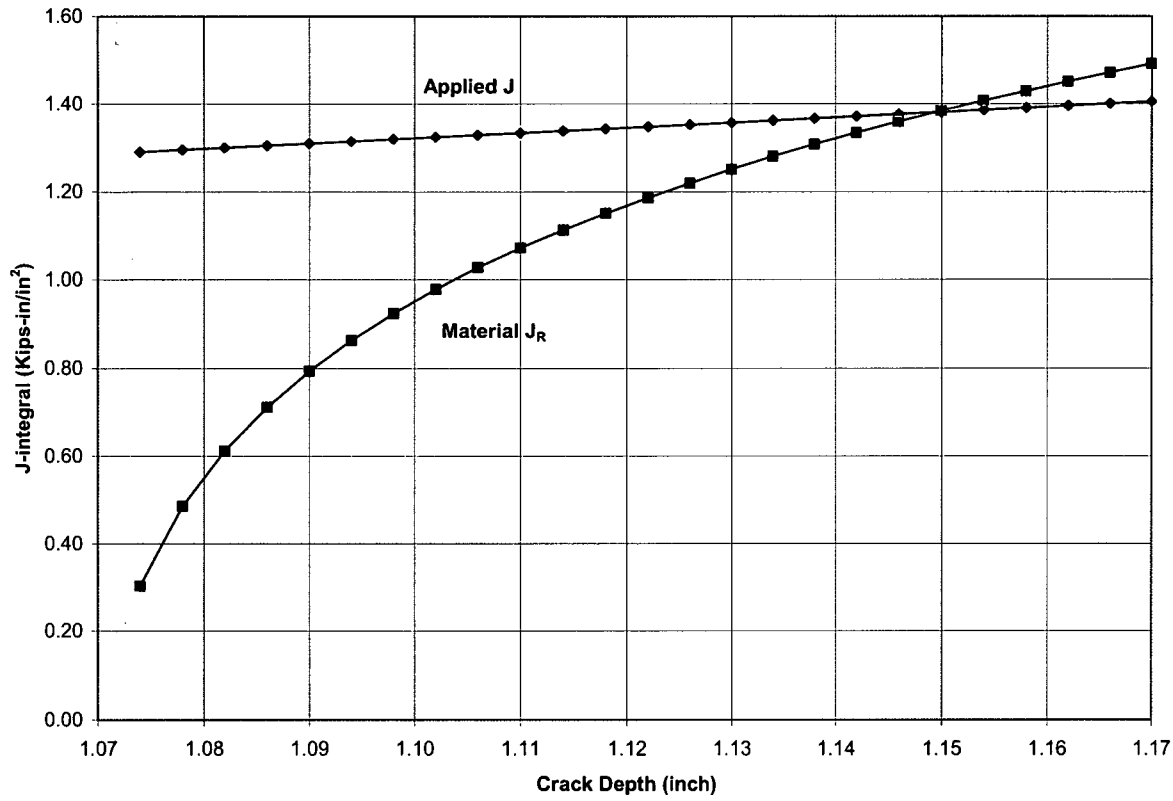

Figure 3-2 Comparison of the Slope of the Applied J-integral and J-R Curve

(Governing Transient: Unit Loading and Unloading)

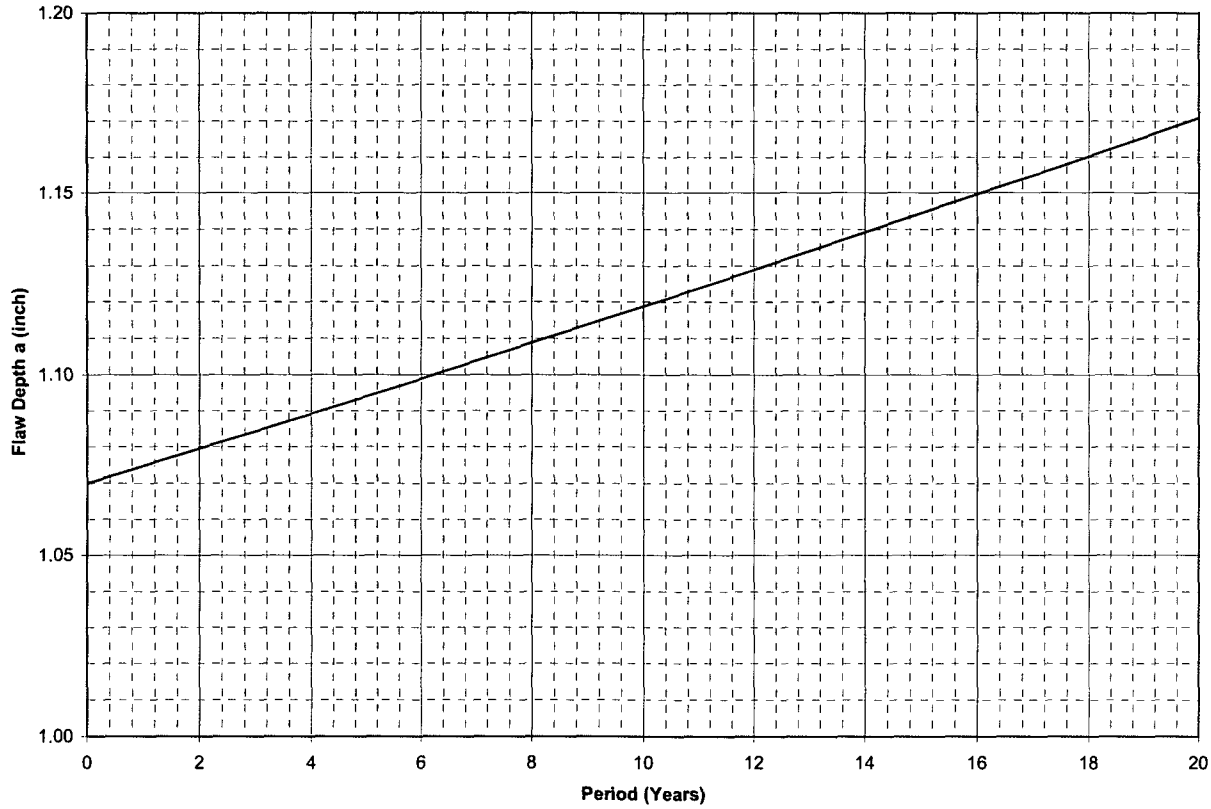

Figure 3-3 Fatigue Crack Growth for the Postulated Flaws in the Head Penetration Nozzle Attachment Welds (Downhill Side)

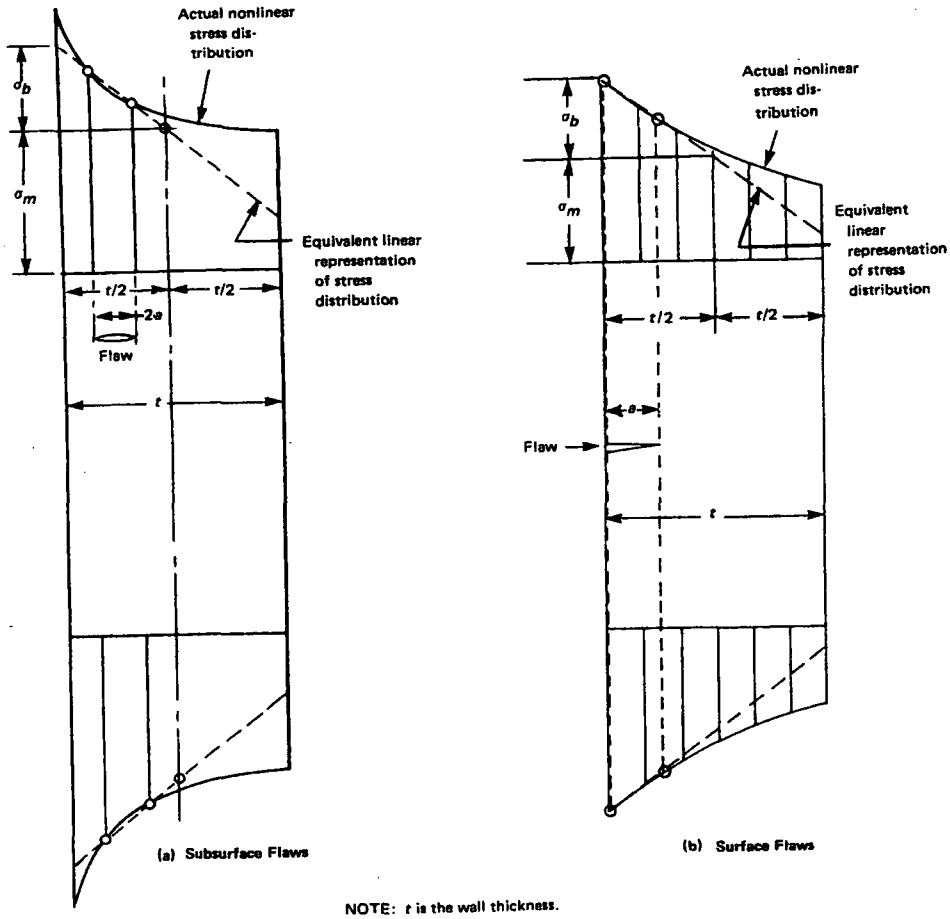

NOTE: t is the wall thickness.

FIG. A-3200-1 LINEARIZED REPRESENTATION OF STRESSES

Figure 3-4 Linearized Representation of Stresses

4 TECHNICAL BASIS FOR "AS-EXCAVATED" REPAIRS

4.1 Introduction

Cracks have been detected on the lower part of the reactor vessel closure head penetration nozzles in some operating plants, both foreign and domestic. Cracks have also been detected in the J-groove attachment welds. The root cause of the problem has been identified as Primary Water Stress Corrosion Cracking (PWSCC) of the Alloy 600 penetration material, or welds.

One of the repair options is to excavate the inside surface of the penetration nozzle on and around each individual crack location. Excavation will serve to remove the material that contains the crack from the penetration nozzle, thus removing the crack.

The purpose of this investigation is to determine the maximum allowable excavation depth and geometry into the penetration nozzle inside surface, which will meet the same ASME Code Section III stress allowables that were used in the reactor vessel stress report for Beaver Valley Unit 2 [12]. In addition, cyclic stresses induced during normal and upset operating conditions are compared against the ASME code fatigue allowable criteria.

4.2 Technical Approach and Acceptance Criteria

A range of excavation sizes in the penetration nozzles was evaluated to determine the maximum depth which meets the ASME Section III stress allowables used in the Beaver Valley Unit 2 reactor vessel stress report [12]. This evaluation was performed for the CRDM penetration nozzles.

The key dimensions of the head penetration nozzles are shown in Table 4-1. The head thickness is 6.188 inches, and the inside radius of the spherical head is 79.094 inches.

The results presented in this section were based on the same evaluation methodology that was used in the Beaver Valley Unit 2 reactor vessel stress report. This report provided the technical basis for the original design compliance with the Section III requirements of the ASME Code. The effects of grind-outs in the regions of interest will be reflected in higher stresses, and the limiting grind-outs will be those which meet the code stress limits.

The design loads include mechanical, thermal, and piping loads. The effect of piping loads in this region is negligible, because the moments are taken out at the location where the penetration exits the vessel head. Thus, the seismic and pipe break loads would be negligible at the location of interest.

The ASME Section III acceptance criteria used in the Beaver Valley Unit 2 reactor vessel stress report are shown in Table 4-2. Calculations were performed for each of the loading conditions. The grind-outs are considered local. The loads and material properties used herein are the same as those used in the original reactor vessel stress report.

Results are provided for the following locations of possible grinding:

1. Penetration nozzles at and above the attachment weld
2. Penetration nozzles below the attachment weld

4.3 Results for the Penetration Nozzles

At and Above the Attachment Welds

For the penetration nozzles, a 360-degree grind out was considered, resulting in a simple thickness reduction in the nozzle. There was no limitation in length. Reducing the nozzle thickness increases the primary stress, and has a small effect on the secondary stress. It was assumed that any grinding performed would have a 3:1 taper or greater, to minimize any stresses from the grinding discontinuity.

For the CRDM penetration nozzle, the required minimum thickness of the nozzle from this evaluation was calculated to be 0.375 inch, so for a nominal thickness of 0.625", the allowable depth of grinding is 0.625"– 0.375" = 0.25 inch. This amounts to a grinding depth of 40 percent of the CRDM penetration nozzle nominal wall thickness.

Below the Attachment Welds

The region of the penetration nozzles below the attachment welds is not part of the pressure boundary, so there are few restrictions on grinding in this region. Also there are no net pressure loads here, so there are no restrictions on the remaining wall thickness. In an extreme case, the entire penetration nozzle below the weld could be removed. If grinding is done in this region, care should be taken to ensure that no sharp corners are created and that the potential for loose part is minimized. The slope of the grinding should be approximately 3:1 to minimize stresses.

4.4 SUMMARY

Allowable grinding depths have been determined for Beaver Valley Unit 2 reactor vessel head penetration nozzles. The approach used is to modify the stresses used in the original stress report to account for various grinding depths, and to determine the maximum depth which would meet the ASME Code Section III requirements.

For the penetration nozzles, grinding can be justified to a depth of 40 percent of the nominal wall thickness for the CRDM penetration nozzles and the minimum required wall thickness is 0.375 inch. For the penetration nozzles below the attachment welds, there are no depth limits on grinding, as this region is within the pressure boundary.

Table 4-1 Key Dimensions of Head Penetration Nozzles		
Penetration Nozzle	**Inside Diameter (in.)**	**Outside Diameter (in.)**
CRDM	2.75	4.00

Table 4-2 Results of Structural Qualification for CRDM housing penetration reduced to 0.375 inch				
Criteria from Ref. [12]	**Category**	**Stress Intensity (ksi)**	**Allowable (ksi)**	**Fatigue Usage Factor**
5.C.1	P_m	12.1	1.0 S_m = 16.6	---
5.C.2	P_L+P_b	24.6	1.5 S_m = 24.9	---
5.C.4	P_L+P_b+Q	55.9[a]	3.0 S_m = 49.8	0.20 [b]
[a] Primary plus secondary membrane plus bending stress intensity, excluding thermal bending stress had been shown to be less than $3S_m$				
[b] Allowable Fatigue Usage Factor is 1.0				

5 SUMMARY AND CONCLUSIONS

As a part of the inspection and repair efforts associated with the reactor vessel head penetration inspection program for Beaver Valley Unit 2, engineering evaluations were performed to support the repair efforts.

The technical basis for the use of the embedded flaw repair method if indications or flaws were found in the head penetration nozzle is provided in Section 2. The fatigue crack growth adjusted allowable flaw sizes for axial and circumferential flaws are provided in Figures 2-7 and 2-10 for the penetration nozzles with repaired flaws.

The technical basis for the use of the embedded flaw repair method if indications or flaws were found in the head penetration attachment welds is provided in Section 3. The results of the evaluation have demonstrated that embedded flaw repair method can be applied to the attachment welds from the inside surface of the vessel head regardless of the sizes of the flaws in the penetration nozzle attachment welds.

The evaluations which address the potential local structural discontinuities resulting from the grinding operations that are performed to excavate flaws in the head penetration nozzle are provided in Section 4. For the penetration nozzles, grinding can be justified to a depth of 40 percent of the nominal wall thickness for the CRDM penetration nozzles and the required minimum wall thickness is 0.375 inch. For the penetration nozzles below the attachment welds, there are no depth limits on grinding, as this region is within the pressure boundary.

6 REFERENCES

1. ASME Code Section XI, "Rules for Inservice Inspection of Nuclear Plant Components," 2001 edition with 2002 Addenda.

2. [ ]a,c,e

3. [ ]a,c,e

4. Regulatory Guide 1.161, "Evaluation of Reactor Pressure Vessel with Charpy Upper-Shelf Energy Less Than 50 ft-lb.

5. [ ]a,c,e

6. [ ]a,c,e

7. Reference Drawings for the J-Weld Dimensions for Beaver Valley Unit 2:

   [ ]a,c,e

8. [ ]a,c,e

9. [ ]a,c,e

10. [ ]a,c,e

11. Marston, T. U. et al., "Flaw Evaluation Procedures: ASME Section XI," Electric Power Research Institute Report EPRI-NP-719-SR, August 1978.

12. [
]a,c,e

13. Reference Drawings for the Control Rod Drive Mechanism for Beaver Valley Unit 2:

[

]a,c,e

14. Fleming, M., et al. "CRDM Nozzle Transient Stress Analysis—Beaver Valley Unit 2 Reactor Vessel Head", Dominion Engineering, Inc. Report R-7779-00-1, Revision 0, August 2003.

15. E. D. Eason, J. E. Wright, E. E. Nelson, "Multivariable Modeling of Pressure Vessel and Piping J-R Data, NUREG/CR-5729, MCS 910401, RF, R5, May 1991.